

# Nesfatin-1 Neurons in Paraventricular and Supraoptic Nuclei of the Rat Hypothalamus Coexpress Oxytocin and Vasopressin and Are Activated by Refeeding

Daisuke Kohno, Masanori Nakata, Yuko Maejima, Hiroyuki Shimizu, Udval Sedbazar, Natsu Yoshida, Katsuya Dezaki, Tatsushi Onaka, Masatomo Mori, and Toshihiko Yada

Division of Integrative Physiology (D.K., M.N., Y.M., U.S., N.Y., K.D., T.Y.), and Division of Brain and Neurophysiology (T.O.), Department of Physiology, Jichi Medical University School of Medicine, Tochigi 329-0498, Japan; and Department of Medicine and Molecular Science (H.S., M.M.), Gunma University Graduate School of Medicine, Gunma 371-8511, Japan

Nesfatin-1, a newly discovered satiety molecule, is located in the hypothalamic nuclei, including the paraventricular nucleus (PVN) and supraoptic nucleus (SON). In this study, fine localization and regulation of nesfatin-1 neurons in the PVN and SON were investigated by immunohistochemistry of neuropeptides and c-Fos. In the PVN, 24% of nesfatin-1 neurons overlapped with oxytocin, 18% with vasopressin, 13% with CRH, and 12% with TRH neurons. In the SON, 35% of nesfatin-1 neurons overlapped with oxytocin and 28% with vasopressin. After a 48-h fast, refeeding for 2 h dramatically increased the number of nesfatin-1 neurons expressing c-Fos immunoreac-

tivity by approximately 10 times in the PVN and 30 times in the SON, compared with the fasting controls. In the SON, refeeding also significantly increased the number of nesfatin-1-immunoreactive neurons and NUCB2 mRNA expression, compared with fasting. These results indicate that nesfatin-1 neurons in the PVN and SON highly overlap with oxytocin and vasopressin neurons and that they are activated markedly by refeeding. Feeding-activated nesfatin-1 neurons in the PVN and SON could play a role in the postprandial regulation of feeding behavior and energy homeostasis. (*Endocrinology* 149: 1295–1301, 2008)

**N**ESFATIN-1, a recently discovered satiety molecule, is distributed in several brain areas implicated in the feeding and metabolic regulation, including the hypothalamic paraventricular nucleus (PVN), supraoptic nucleus (SON), arcuate nucleus, lateral hypothalamic area, and nucleus tractus solitarius in the brain stem (1–4). Intracerebroventricular (icv) administration of nesfatin-1 and NEFA/nucleobinding-2 (NUCB2), a precursor of nesfatin-1, suppresses food intake, whereas icv administration of anti-nesfatin-1 antibody increases food intake (1). Nesfatin-1 suppresses feeding in a leptin-independent manner; nesfatin-1 antibody did not inhibit leptin-induced satiety and nesfatin-1 suppresses food intake in Zucker rats whose leptin receptor is mutated (1).

Both NUCB2 mRNA level and nesfatin-1 concentration in the PVN significantly decrease after 24 h starvation as compared with *ad libitum* (1). This suggests that nesfatin-1 in the PVN could play a role in satiety and, possibly, energy homeostasis after meal intake. In the PVN, several distinct endogenous peptides (CRH, oxytocin, TRH, and vasopressin) inhibit food intake (5–8). In the PVN and SON, nesfatin-1-immunoreactive neurons were colocalized with oxytocin and vasopressin (2). Therefore, possible interaction between

the neurons containing these neuropeptides and nesfatin-1 neurons in the PVN and SON could be implicated in the regulation of feeding and metabolism. In this study, therefore, we investigated colocalization of nesfatin-1 with classical neuropeptides of the PVN and SON and explored the regulation of nesfatin-1 neurons by refeeding.

## Materials and Methods

### Animals

Adult (7–9 wk old) male Sprague Dawley rats were maintained on a 12-h light, 12-h dark cycle and given conventional food (CE-2; Clea, Osaka, Japan) and water *ad libitum*. The animal protocols for this study were approved by the Jichi Medical University Institute of Animal Care and Use Committee and were in accordance with the Japanese Physiological Society's guidelines for animal care.

### Tissue preparation for immunohistochemistry

Rats were deeply anesthetized with urethane (1 g/kg, ip) and were perfused transcardially with saline containing heparin (20 U/ml) for 3 min and then 4% paraformaldehyde in 0.1 M phosphate buffer (PB) for 20 min. The brains were removed and postfixed in the same fixative for 1 h and in 4% paraformaldehyde in 0.1 M PB containing 15% sucrose overnight at 4 C. They were then transferred to 30% sucrose solution in 0.1 M PB for 2 d. The brains were frozen on dry ice and kept at –80 C until sectioning. Coronal sections (40  $\mu$ m) of the hypothalamus were cut using a freezing microtome and collected at 160- $\mu$ m intervals.

For the immunohistochemistry of TRH and CRH, rats received an icv injection of colchicine before perfusion. One day before perfusion, rats were anesthetized by injection of Avertin (tribromoethanol, 200 mg/kg, ip) and placed in a stereotaxic frame (DAVID Kopf Instruments, Tujunga, CA), and a stainless steel guide cannula (26-gauge) was inserted into the brain with the tip in the right lateral ventricle; 0.8 mm caudal and 1.6 mm right to the bregma and 3.5 mm below the skull, and then colchicine (0.2 mg/15  $\mu$ l/animal dissolved in saline) was injected into the lateral ventricle through a 30-gauge injection needle.

First Published Online November 29, 2007

Abbreviations: DAB, Diaminobenzidine; icv, intracerebroventricular; NMU, neuromedin U; NUCB2, nucleobinding-2; PB, phosphate buffer; PVN, paraventricular nucleus; RT, room temperature; SON, supraoptic nucleus.

*Endocrinology* is published monthly by The Endocrine Society (<http://www.endo-society.org>), the foremost professional society serving the endocrine community.

### Triple-labeling immunohistochemistry for nesfatin-1, oxytocin, and vasopressin

Sections were rinsed in PBS (0.01 M PB and 0.9% NaCl) and then blocked with 1% BSA, 1% normal goat serum and 0.1% Triton X-100 in PBS for 1 h. Then they were incubated with first antibodies, rabbit anti-nesfatin-1 antibody (Gunma University; 1:1000) (1), mouse anti-oxytocin monoclonal antibody (MAB5296; Chemicon, Temecula, CA; 1:600), and guinea pig anti-Arg8-vasopressin antiserum (T-5048; Peninsula Laboratories, San Carlos, CA; 1:2000), diluted in blocking solution for overnight at room temperature (RT). After rinsing, sections were incubated with secondary antibodies, Alexa 488 goat antirabbit IgG, Alexa 350 goat antimouse IgG, and Alexa 594 goat anti-guinea pig IgG (Molecular Probes, Carlsbad, CA; 1:500) for 40 min. Slices were then rinsed, mounted on slides, and coverslipped with fluorescent mounting medium (DakoCytomation, Carpinteria, CA). Before performing the triple- and double-labeling immunohistochemistry, each primary antibody was tested separately, and immunohistochemical control included omission of primary antibodies in each case. Fluorescence images were acquired with a BX50 microscope and a DP50 digital camera (Olympus, Tokyo, Japan). Using Photoshop (Adobe, San Jose, CA), brightness and contrast were adjusted, and fluorescence photographs were combined to visualize double- or triple-labeled cells by the screen blending mode. To count fluorescence, one combined photograph from each 40- $\mu$ m slice was used.

### Double-labeling immunohistochemistry for nesfatin-1 and TRH or CRH

For double-labeling immunohistochemistry for nesfatin-1 and TRH or CRH, we used anti-nesfatin-1, anti-TRH, and anti-CRH antisera raised in rabbits. To eliminate the possible cross-reactivity, a modification of recently described protocol was used (9, 10). Briefly, the sections were rinsed and then blocked. Sections were incubated with a rabbit primary antiserum against nesfatin-1 (1:100,000) or TRH (11170; Progen Biotechnik, Heidelberg, Germany; 1:5,000) overnight at RT. Sections were rinsed and incubated with biotinylated goat antirabbit IgG (Vector Laboratories, Burlingame, CA; 1:500) for 30 min and were incubated with ABC reagent (Vector Laboratories; 1:500) for 30 min. Then sections were rinsed in buffer of 0.1 M Tris-HCl (pH 7.5), 0.15 M NaCl, and 0.05% Tween 20 and blocked with 0.05% blocking reagent (PerkinElmer, Waltham, MA). Then sections were treated with biotinyl tyramide (PerkinElmer 1:50) diluted in amplification reagent (PerkinElmer) for 5 min. After rinse in buffer of 0.1 M Tris-HCl (pH 7.5), 0.15 M NaCl, and 0.05% Tween 20, sections were incubated with streptavidin-Alexa 488 conjugate (Molecular Probes; 1:500) diluted in blocking reagent for 40 min. After a rinse in PBS, sections were incubated with a primary rabbit antiserum against CRH (T-4037; Peninsula Laboratories; 1:1000) or nesfatin-1 (1:1000) overnight, rinsed, and incubated with Alexa 594 goat-antirabbit IgG (Molecular Probes; 1:500) for 40 min. After treatment with first primary antibodies against nesfatin-1 (1:100,000) or TRH (1:5,000), the treatment with Alexa 594 goat-antirabbit IgG resulted in no staining.

### Acquirement of confocal images

Double-labeling immunohistochemistry for nesfatin-1 and oxytocin was done by following the procedure. Sections were blocked and incubated with rabbit anti-nesfatin-1 antibody and mouse anti-oxytocin monoclonal antibody as first antibodies, as described above. Then sections were incubated with secondary antibodies, Alexa 488 goat antirabbit IgG, and Alexa 594 goat antimouse IgG (Molecular Probes; 1:500) for 40 min. The other double-labeling immunohistochemistries were done by the same procedure as described above. Confocal fluorescence images were acquired with a confocal laser-scanning microscope (Fluoview FV300-TP; Olympus).

### Double-labeling immunohistochemistry for c-Fos and nesfatin-1 in ad libitum-fed, fasted, and refed rats

For the study under fasting and refeeding conditions, food deprivation for 48 h was followed by 2 h refeeding that started at the beginning of the dark phase. Two hours after the beginning of the dark phase, rats were anesthetized and fixed, and brain sections were prepared as de-

scribed. Sections were rinsed in PBS and then incubated in 0.3% H<sub>2</sub>O<sub>2</sub> for 20 min. After rinsing, sections were blocked for 30 min and incubated with rabbit anti-c-Fos antibody (Ab-5; Calbiochem, San Diego, CA; 1:100,000) overnight at RT. Then the sections were rinsed and incubated with biotinylated goat antirabbit IgG for 30 min. After the rinse, sections were incubated with ABC reagent for 30 min (Vector Laboratories; 1:500). After the rinse in PBS and 0.175 M sodium acetate buffer (pH 5.6), color was developed with a nickel-diaminobenzidine (DAB) solution (10 g/liter nickel ammonium sulfate, 0.2 g/liter DAB, and 0.006% H<sub>2</sub>O<sub>2</sub> in sodium acetate buffer) for 5 min.

After the rinse in PBS, sections were treated with an avidin and biotin blocking solution (Vector Laboratories) and then incubated with rabbit anti-nesfatin-1 antibody (1:5000) diluted in a blocking solution overnight at RT. After the rinse, sections were incubated with biotinylated goat antirabbit antibody for 30 min and incubated in ABC reagent for 30 min. Then the sections were rinsed in PBS and Tris-buffered saline [0.1 M Tris-HCl (pH 7.4), 0.15 M NaCl], and color was developed with a DAB solution (0.2 g/liter DAB and 0.006% H<sub>2</sub>O<sub>2</sub> in Tris-buffered saline). Slices were then rinsed, mounted on slides, and coverslipped with Entellan new (Merck, Darmstadt, Germany).

### Real-time RT-PCR analysis

Two hours after the beginning of the dark phase, rats were deeply anesthetized with urethane and decapitated, and their brains were removed. Brain slices containing the entire SON were prepared, and the entire SON was excised from the left and right sides. Total RNA of SON was isolated using TRIzol (Invitrogen, Carlsbad, CA) and treated with RQ1-DNase (Promega, Madison, WI) to remove residual contaminations with DNA. First-strand cDNA synthesis was completed using ReverTra Ace (Toyobo, Osaka, Japan). Primers for real-time PCR were first examined by HotStarTaq DNA polymerase (94 C for 15 sec, 60 C for 20 sec, and 72 C for 20 sec  $\times$  30 cycles; QIAGEN, Hilden, Germany) and agarose gel electrophoresis for correct product size and absence of primer-dimer formation. Using a QuantiTect SYBR Green PCR kit (QIAGEN), real-time PCRs (95 C for 15 sec, 60 C for 20 sec, and 72 C for 20 sec  $\times$  40 cycles) were performed in an ABI-Prism 7700 sequence detector (Applied Biosystems, Foster City, CA). Product accumulation was measured in real time, and the mean cycle threshold (the cycle during which the product is first detected) was determined for replicate samples ( $n = 8$  or  $9$  independent reactions per primer pair and cDNA sample) run on the same plate. Different cDNA samples were normalized using primer sets to the housekeeping gene glyceraldehydes-3-phosphate dehydrogenase. Primers were as follows: glyceraldehydes-3-phosphate dehydrogenase, 5'-GGCACAGTCAAGGCTGAGAATG-3' and 5'-ATGGTGGTGAA-GACGCCAGTA-3'; NUCB2, 5'-TGGAAACAGATCCGCATTTCAG-3' and 5'-CAGTTCATCCAGTCTCGTCTCTCAC-3'.

### Data presentation and statistical analysis

Data are presented as the mean  $\pm$  SE. Each study was based on at least three rats. Data were analyzed by one-way ANOVA and differences were evaluated by Fisher's protected least significant difference. Values of  $P < 0.05$  were considered significant.

## Results

### Nesfatin-1 neurons were colocalized with oxytocin, vasopressin, CRH, and TRH neurons in the PVN

In the PVN, nesfatin-1, oxytocin, and vasopressin-immunoreactive neurons were identified by Alexa 488 (green), 350 (blue), and 594 (red) fluorescence, respectively (Fig. 1, A–C). Total  $534.5 \pm 136.7$  ( $n = 4$ ) nesfatin-1-immunoreactive neurons were found in PVN, in which  $127.0 \pm 30.5$  ( $n = 4$ ) (24%) neurons were oxytocin-immunoreactive (light blue and white),  $95.0 \pm 19.0$  ( $n = 4$ ) (18%) were vasopressin-immunoreactive (yellow and white), and  $42.0 \pm 10.2$  ( $n = 4$ ) (8%) were both oxytocin and vasopressin immunoreactive (white) (Fig. 1). Conversely,  $127.0 \pm 30.5$  of  $318.0 \pm 42.4$  ( $n = 4$ ) (40%) oxytocin-immunoreactive neurons were nesfatin-1-immuno-

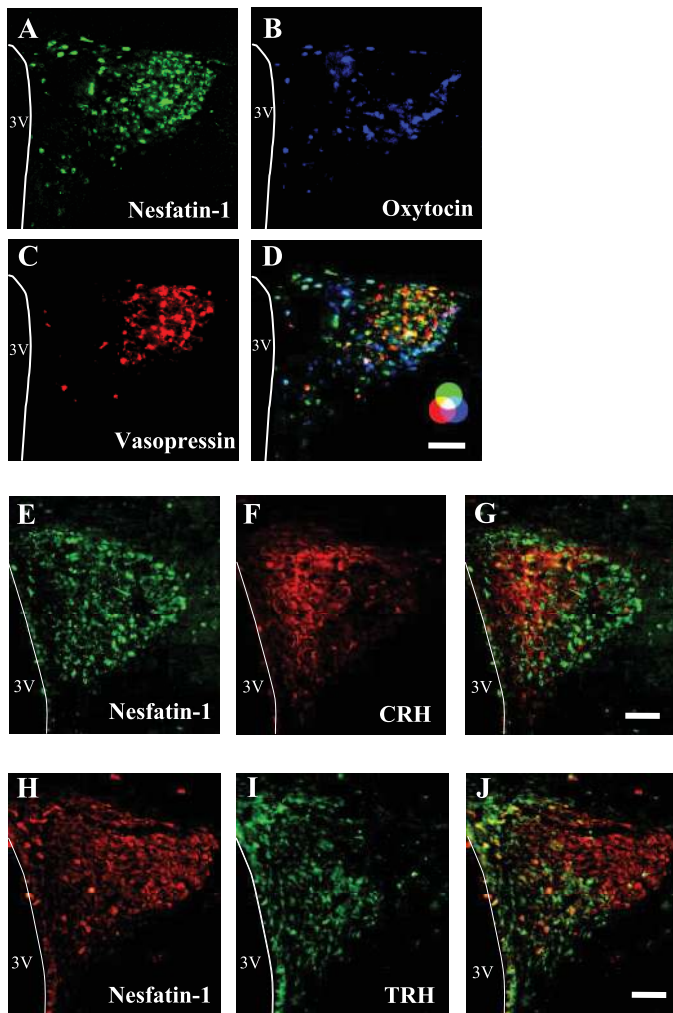


FIG. 1. Colocalization of nesfatin-1 neurons with oxytocin, vasopressin, CRH, and TRH neurons in PVN. A–D, Nesfatin-1-immunoreactive neurons (green) (A), oxytocin-immunoreactive neurons (blue) (B), and vasopressin-immunoreactive neurons (red) (C) are shown. D, Colocalization of nesfatin-1 and oxytocin neurons (light blue), nesfatin-1 and vasopressin neurons (yellow), oxytocin and vasopressin neurons (pink), and nesfatin-1, oxytocin, and vasopressin neurons (white) are shown. E–G, Nesfatin-1-immunoreactive neurons (green) (E), CRH-immunoreactive neurons (red) (F), and colocalization (yellow) (G) are shown. H–J, Nesfatin-1-immunoreactive neurons (red) (H), TRH-immunoreactive neurons (green) (I), and colocalization (yellow) (J) are shown. Scale bar, 100  $\mu$ m. 3V, Third ventricle.

reactive, and  $95.0 \pm 19.0$  of  $201.5 \pm 22.0$  (47%) ( $n = 4$ ) vasopressin-immunoreactive neurons were nesfatin-1 immunoreactive. Furthermore, confocal analysis detected the colocalization of nesfatin-1 with oxytocin and vasopressin in the PVN with higher resolution (Fig. 2, A–C and G–I).

We also investigated the colocalization of nesfatin-1 with CRH or with TRH in the neurons of the PVN. Nesfatin-1 neurons were identified by Alexa 488 fluorescence (green) and CRH neurons by Alexa 594 fluorescence (red) (Fig. 1, E and F). Total  $431.4 \pm 76.6$  ( $n = 3$ ) nesfatin-1-immunoreactive neurons were found in PVN, in which  $54.7 \pm 16.8$  ( $n = 3$ ; 13%) neurons were CRH immunoreactive (yellow) (Fig. 1G). Conversely,  $54.7 \pm 16.8$  of  $412.2 \pm 39.0$  ( $n = 3$ ; 13%) CRH-immunoreactive neurons were nesfatin-1 immunoreactive.

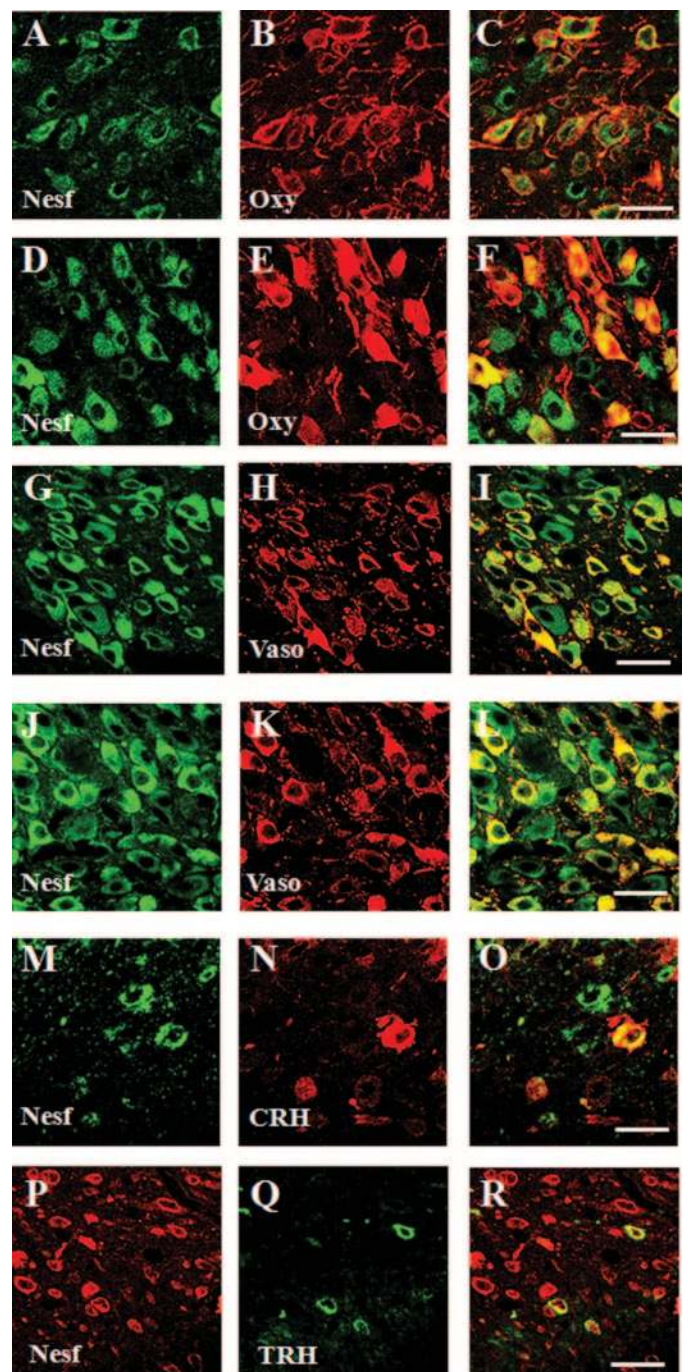


FIG. 2. Confocal images showing colocalization of nesfatin-1 (Nesf) with oxytocin (Oxy), vasopressin (Vaso), CRH, and TRH in neurons of PVN and SON. Nesfatin-1-immunoreactive neurons (A, D, G, J, M, and P), oxytocin-immunoreactive neurons in PVN (B) and SON (E), vasopressin-immunoreactive neurons in PVN (H) and SON (K), CRH-immunoreactive neurons in PVN (N), TRH-immunoreactive neurons in PVN (Q), and their merges (C, F, I, L, O, and R) are shown. Scale bar, 30  $\mu$ m.

Furthermore, confocal analysis revealed fine colocalization of nesfatin-1 and CRH (Fig. 2, M–O). Next, nesfatin-1 neurons were identified by Alexa 594 fluorescence (red), and TRH neurons by Alexa 488 fluorescence (green) (Fig. 1, H and I). Total  $504.0 \pm 59.6$  ( $n = 3$ ) nesfatin-1-immunoreactive

neurons were found in PVN, in which  $59.1 \pm 16.5$  ( $n = 3$ ; 12%) neurons were TRH immunoreactive (yellow) (Fig. 1J). Conversely,  $59.1 \pm 16.5$  of  $219.1 \pm 76.9$  (27%;  $n = 3$ ) TRH-immunoreactive neurons were nesfatin-1 immunoreactive. Colocalization of nesfatin-1 and TRH was confirmed in confocal images (Fig. 2, P–R).

*Nesfatin-1 neurons were colocalized with oxytocin and vasopressin neurons in the SON*

In the SON, the nesfatin-1, oxytocin, and vasopressin-immunoreactive neurons were identified by Alexa 488 (green), 350 (blue), and 594 (red) fluorescence, respectively (Fig. 3, A–C). Total  $440.0 \pm 71.2$  ( $n = 4$ ) nesfatin-1-immunoreactive neurons were found in SON, in which  $153.5 \pm 32.1$  ( $n = 4$ ; 35%) neurons were oxytocin immunoreactive (light blue and white),  $124.5 \pm 28.8$  ( $n = 4$ ; 28%) were vasopressin immunoreactive (yellow and white), and  $25.3 \pm 6.1$  ( $n = 4$ ; 6%) were immunoreactive to both oxytocin and vasopressin (white) (Fig. 3D). Conversely,  $153.5 \pm 32.1$  of  $310.3 \pm 25.9$  ( $n = 4$ ; 49%) oxytocin-immunoreactive neurons and  $124.5 \pm 28.8$  of  $210.0 \pm 30.7$  ( $n = 4$ ; 59%) vasopressin-immunoreactive neurons were nesfatin-1 immunoreactive. Confocal analysis detected fine colocalization of nesfatin-1 with oxytocin and vasopressin in the SON (Fig. 2, D–F and J–L).

*Refeeding induced c-Fos expression in nesfatin-1 neurons of the PVN and SON*

After refeeding for 2 h following 48 h fasting, c-Fos-immunoreactive neurons were observed abundantly in the SON, PVN, dorsomedial hypothalamic nucleus, and preoptic area and to a lesser extent in the arcuate nucleus of the hypothalamus. In the PVN, c-Fos immunoreactivity was observed in  $90.7 \pm 24.7$  ( $n = 3$ ) nesfatin-1-immunoreactive neurons in *ad libitum* conditions,  $22.0 \pm 7.0$  ( $n = 5$ ) neurons in fasting conditions, and  $211.4 \pm 56.3$  ( $n = 5$ ) neurons in refeeding conditions (Fig. 4, A–E). The number of nesfatin-1 neurons expressing c-Fos immunoreactivity was signifi-

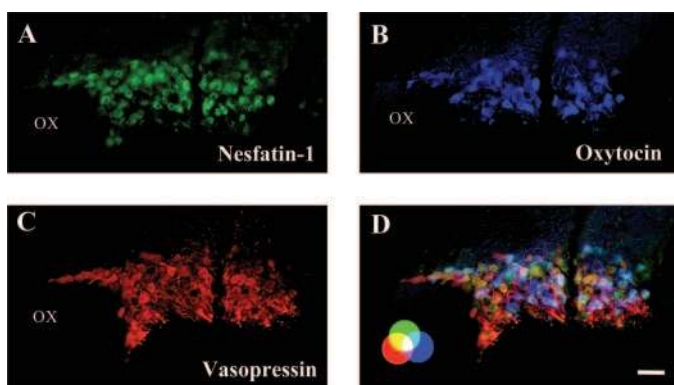


FIG. 3. Colocalization of nesfatin-1, oxytocin, and vasopressin neurons in SON. Nesfatin-1-immunoreactive neurons (green) (A), oxytocin-immunoreactive neurons (blue) (B), and vasopressin-immunoreactive neurons (red) (C) are shown. D, Colocalization of nesfatin-1 and oxytocin neurons (light blue), nesfatin-1 and vasopressin neurons (yellow), oxytocin and vasopressin neurons (pink), and nesfatin-1, oxytocin, and vasopressin neurons (white) are shown. Scale bar, 50  $\mu$ m. ox, Optic chiasm.

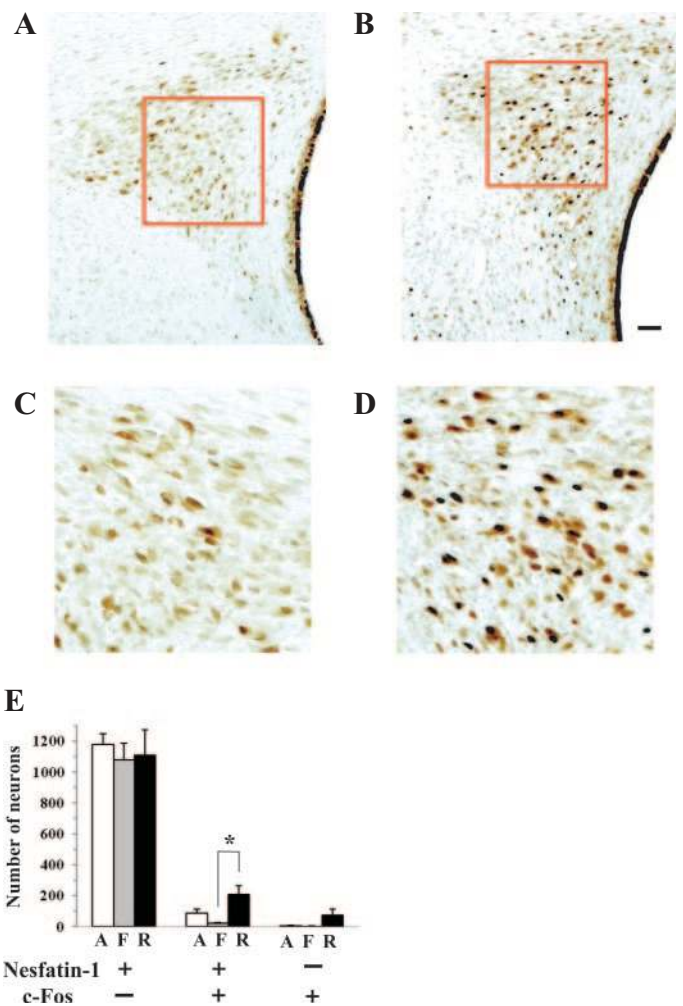


FIG. 4. c-Fos expression on nesfatin-1 neurons in PVN after refeeding. Double-immunohistochemical staining of c-Fos (black) and nesafatin-1 (brown) in PVN after 48 h fasting (panels A and C) and after 2 h refeeding following 48 h fasting (panels B and D). Scale bar, 50  $\mu$ m. Panels C and D, Magnification of the areas in panels A and B marked by red squares. Panel E, The number of c-Fos-immunoreactive neurons on nesfatin-1-immunoreactive neurons in PVN was significantly (\*,  $P < 0.005$ ) higher in refeeding than fasting conditions. A, *Ad libitum*; F, fasting; R, refeeding.

cantly (10 times,  $P < 0.005$ ) greater under refeeding, compared with fasting conditions (Fig. 4E).

In the SON, c-Fos-immunoreactivity was observed in  $155.7 \pm 34.9$  ( $n = 3$ ) nesfatin-1-immunoreactive neurons in *ad libitum* conditions,  $26.0 \pm 21.5$  ( $n = 5$ ) neurons in fasting conditions, and  $799.8 \pm 162.5$  ( $n = 5$ ) neurons in refeeding conditions (Fig. 5, A–E). Thus, the number of c-Fos-positive nesfatin-1 neurons was dramatically elevated by refeeding, compared with *ad libitum* (5 times,  $P < 0.005$ ) and fasting conditions (31 times,  $P < 0.0005$ ) (Fig. 5E). Total number of nesfatin-1 immunoreactive neurons in the SON was significantly increased by refeeding ( $1443.0 \pm 174.5$  neurons,  $n = 5$ ), compared with *ad libitum* ( $865.3 \pm 87.9$  neurons,  $n = 5$ ,  $P < 0.05$ ) and fasting conditions ( $538.4 \pm 70.4$  neurons,  $n = 5$ ,  $P < 0.0005$ ) (Fig. 5F). Relative ratios of NUCB2 mRNA expression in the SON were significantly decreased ( $P < 0.005$ ) in fasting ( $0.144 \pm 0.013$ ,  $n = 9$ ), compared with *ad libitum* ( $0.503 \pm$

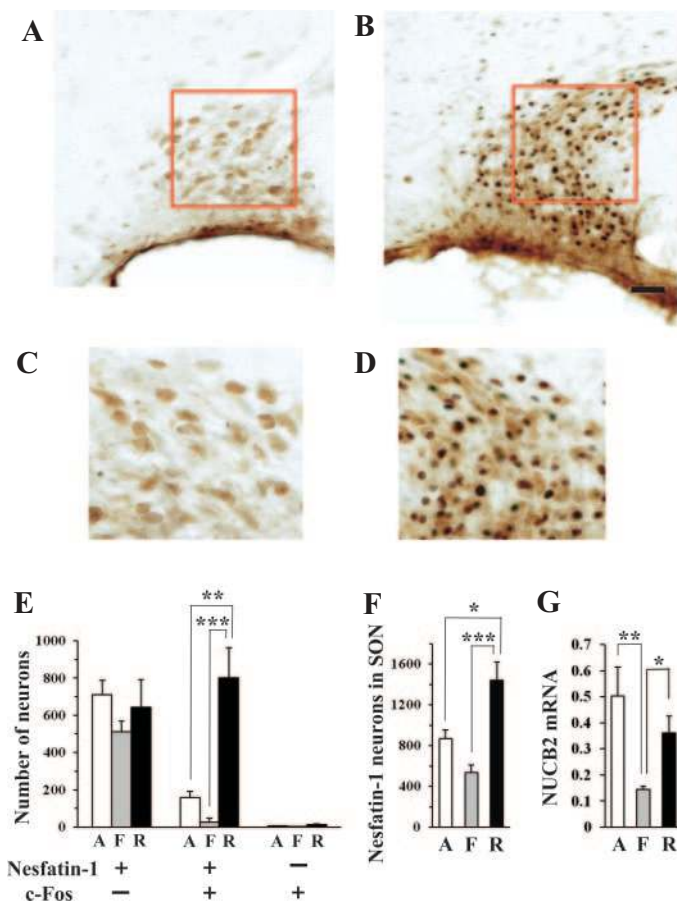


FIG. 5. C-Fos expression on nesfatin-1 neurons in SON after refeeding. Double-immunohistochemical staining of c-Fos (black) and nesfatin-1 (brown) in SON after 48 h fasting (panels A and C) and after 2 h refeeding following 48 h fasting (panels B and D). Scale bar, 50  $\mu$ m. Panels C and D, Magnification of the areas in panels A and B marked by red squares. Panel E, The number of c-Fos-immunoreactive neurons in nesfatin-1-immunoreactive neurons in SON was significantly greater under refeeding than *ad libitum* (\*\*,  $P < 0.005$ ) and fasting (\*\*\*,  $P < 0.0005$ ) conditions. Panel F, The number of total nesfatin-1-immunoreactive neurons in SON was significantly larger in refeeding than *ad libitum* (\*,  $P < 0.05$ ) and fasting (\*\*\*,  $P < 0.0005$ ) conditions. Panel G, NUCB2 mRNA expressions in SON in *ad libitum* condition significantly (\*\*,  $P < 0.005$ ) decreased in fasting, and it was significantly (\*,  $P < 0.05$ ) increased in refeeding. A, *Ad libitum*; F, fasting; R, refeeding.

0.110,  $n = 8$ ), and increased ( $P < 0.05$ ) by refeeding ( $0.361 \pm 0.064$ ,  $n = 9$ ), compared with fasting (Fig. 5G).

### Discussion

In this study, we found that nesfatin-1 neurons are abundant in the PVN and SON and that they overlap extensively with oxytocin and vasopressin neurons and, to a lesser extent, with CRH and TRH neurons. Our finding not only confirmed the recent report (2) but also substantiated the observation by quantitative analysis. Refeeding after fasting dramatically increased the number of nesfatin-1 neurons that express c-Fos immunoreactivity in the PVN and SON. In the SON, refeeding also increased the number of nesfatin-1-immunoreactive neurons and mRNA expression of NUCB2. These findings suggest that nesfatin-1

neurons in the PVN and SON, possibly via interaction with oxytocin and vasopressin neurons, may play a role in the postprandial regulation of the feeding behavior and peripheral metabolism.

It has recently been reported that nesfatin-1 is colocalized with oxytocin and vasopressin in the PVN (2). In this study, we quantified the colocalization of nesfatin-1 with oxytocin, vasopressin, CRH, and TRH in the PVN. Among these neuropeptides, CRH is thought to be implicated in anorexia nervosa and the feeding suppression under stress conditions (11). Therefore, the specific subtype of nesfatin-1 neuron that coexpresses CRH in the PVN could be involved in the potent anorectic effect of nesfatin-1. However, the incidence of this subtype of nesfatin-1 neuron is modest (13%). In contrast, as much as 24% of the PVN nesfatin-1 neurons coexpress oxytocin. Furthermore, 40% of the PVN oxytocin neurons contain nesfatin-1. The finding that nesfatin-1 and oxytocin neurons highly overlap in the PVN might imply possible functional association between nesfatin-1 and oxytocin. It has been reported that the parvocellular PVN oxytocin neurons project to the nucleus tractus solitarius, the site at which central and peripheral signals are integrated, and that this neuronal pathway is related to inhibition of food intake (12, 13). Collectively, the PVN nesfatin-1/oxytocin neurons could also be involved in the anorectic nesfatin-1 pathway.

It was previously reported that an icv injection of  $\alpha$ -MSH increases NUCB2 mRNA expression in the PVN, suggesting that nesfatin-1 neurons in the PVN could function downstream of melanocortin pathway (1). However, underlying mechanisms have remained unknown. We found that nesfatin-1 in the PVN is colocalized with oxytocin, vasopressin, CRH, and TRH, the substances that are thought to work at downstream of melanocortin pathway: central administration of  $\alpha$ -MSH activates oxytocin, CRH, and TRH neurons (13–15) and stimulates vasopressin release in PVN (16). Melanocortin-4 receptors, the principal receptor that mediates anorectic effects of  $\alpha$ -MSH, are distributed abundantly in the PVN (17, 18). The melanocortin-4 receptors located in the PVN are important for the feeding regulation (19). Collectively, we speculate that the PVN nesfatin-1-neurons coexpressing oxytocin, vasopressin, CRH, or TRH could serve as an effector of melanocortin signaling.

It was shown that the refeeding-induced c-Fos expression in the ventral parvocellular subdivision of PVN depends on melanocortin signal (20). Hence, our results could be interpreted that refeeding influenced proopiomelanocortin neurons, which in turn evoked c-Fos in nesfatin-1 neurons. Neuromedin U (NMU) could also be upstream of nesfatin-1 because an icv injection of NMU increases c-Fos expression in the SON and PVN (21, 22), and NMU induces satiety in a leptin-independent manner similarly to nesfatin-1 (23).

Refeeding (24) and scheduled food intake (25) increase c-Fos expression in the SON and PVN. We not only confirmed this previous report but also identified a novel neuron subtype as the target: refeeding markedly stimulates c-Fos expression in nesfatin-1-immunoreactive neurons in the SON and PVN.

In the SON, furthermore, c-Fos-expression occurs primarily in nesfatin-1-immunoreactive neurons. It was shown that the c-Fos expressing neurons in the SON after refeeding are mainly vasopressin neurons (24). Therefore, it is likely that at least a fraction of c-Fos-expressing nesfatin-1 neurons in the SON, observed in the present study, coexpresses vasopressin. Although physiological roles of the nesfatin-1 neurons coexpressing vasopressin remain unknown, it could be related to the metabolic effects of vasopressin: peripheral injection of vasopressin suppresses food intake (8), and vasopressin-1a receptor knockout mice exhibit abnormalities in lipid metabolism (26), glucose homeostasis (27), and blood pressure (28). In the PVN, refeeding induces c-Fos expression in not only magnocellular neurons containing vasopressin neurons but also parvocellular neurons containing CRH neurons (24). Parvocellular nesfatin-1 neurons could also be related to the postrefeeding functions.

It should be noted that, although our protocol of 48 h fasting and 2 h refeeding has been used widely as the condition of hunger and satiety, the additional and/or complex physiological effects cannot be excluded. Stress can be induced by food deprivation (29), and icv administration of stress-related hormones, NMU, induces c-Fos expression in the PVN and SON (21, 22). Therefore, the c-Fos induction in nesfatin-1 neurons could underlie stress-related functions other than feeding. Furthermore, the PVN and SON are implicated in the homeostasis of water balance (30), a function that can secondarily influence food intake (31).

In this study, the amount of NUCB2 mRNA expression and the number of nesfatin-1-immunoreactive neurons also changed on fasting and refeeding. It is reported that the mRNA expression of NUCB2 in the pancreatic islets increases more than 5 times in the high-fat diet-fed mice, compared with normal diet conditions (32). Hence, acute and chronic metabolic states may affect the expression of NUCB2 mRNA and nesfatin-1.

This study demonstrated that nesfatin-1 neurons in the PVN and SON overlap extensively with oxytocin and vasopressin neurons and that refeeding highly selectively activates nesfatin-1 neurons in the PVN and SON and increases nesfatin-1 expression in the SON. These findings suggest a hypothesis that nesfatin-1 neurons in the PVN and SON play a role in the postprandial regulation of feeding and energy homeostasis. To verify this hypothesis, functional interaction of nesfatin-1 with oxytocin, vasopressin, and other neuropeptides in the PVN and SON needs to be clarified.

### Acknowledgments

We thank Dr. Tom Kouki for technical advice.

Received September 17, 2007. Accepted November 20, 2007.

Address all correspondence and requests for reprints to: Dr. Toshiko Yada, Division of Integrative Physiology, Department of Physiology, Jichi Medical University, School of Medicine, Tochigi 329-0498, Japan. E-mail: tyada@jichi.ac.jp.

This work was supported by a Grant-in-Aid for Scientific Research (B) and that on Priority Areas (15081101) from the Japan Society for the Promotion of Science, a grant from the 21st century Center of Excellence

program, a grant from the Science Research Promotion Fund from the Promotion and Mutual Aid Corporation for Private Schools of Japan, an Insulin Research Award from Novo Nordisk Pharma Ltd., a grant from the Japan Diabetes Foundation, and a grant from the Smoking Research Foundation (to T.Y.), and a Research Award to Jichi Medical University (JMU) Graduate Student (to D.K.).

Disclosure Statement: The authors have nothing to disclose.

### References

- Oh-I S, Shimizu H, Satoh T, Okada S, Adachi S, Inoue K, Eguchi H, Yamamoto M, Imaki T, Hashimoto K, Tsuchiya T, Monden T, Horiguchi K, Yamada M, Mori M 2006 Identification of nesfatin-1 as a satiety molecule in the hypothalamus. *Nature* 443:709–712
- Brailoiu GC, Dun SL, Brailoiu E, Inan S, Yang J, Chang JK, Dun NJ 2007 Nesfatin-1: distribution and interaction with a G protein-coupled receptor in the rat brain. *Endocrinology* 148:5088–5094
- Cowley MA, Grove KL 2006 To be or NUCB2, is nesfatin the answer? *Cell Metab* 4:421–422
- Schwartz MW, Woods SC, Porte Jr D, Seeley RJ, Baskin DG 2004 Central nervous system control of food intake. *Nature* 404:661–671
- Olson BR, Drutarosky MD, Stricker EM, Verbalis JG 1991 Brain oxytocin receptor antagonism blunts the effects of anorexigenic treatments in rats: evidence for central oxytocin inhibition of food intake. *Endocrinology* 129:785–791
- Richard D, Huang Q, Timofeeva E 2000 The corticotropin-releasing hormone system in the regulation of energy balance in obesity. *Int J Obes Relat Metab Disord* 24:S36–S39
- Kow LM, Pfaff DW 1991 The effects of the TRH metabolite cyclo(His-Pro) and its analogs on feeding. *Pharmacol Biochem Behav* 38:359–364
- Langhans W, Delprete E, Scharer E 1991 Mechanisms of vasopressin's anorectic effect. *Physiol Behav* 49:169–176
- Cota D, Proulx K, Smith KA, Kozma SC, Thomas G, Woods SC, Seeley RJ 2006 Hypothalamic mTOR signaling regulates food intake. *Science* 312:927–930
- Hunyady B, Krempels K, Harta G, Mezey E 1996 Immunohistochemical signal amplification by catalyzed reporter deposition and its application in double immunostaining. *J Histochem Cytochem* 44:1353–1362
- Connan F, Lightman SL, Landau S, Wheeler M, Treasure J, Campbell IC 2007 An investigation of hypothalamic-pituitary-adrenal axis hyperactivity in anorexia nervosa: the role of CRH and AVP. *J Psychiatr Res* 41:131–143
- Blevins JE, Schwartz MW, Baskin DG 2004 Evidence that paraventricular nucleus oxytocin neurons link hypothalamic leptin action to caudal brain stem nuclei controlling meal size. *Am J Physiol Regul Integr Comp Physiol* 287:R87–R96
- Sabatier N 2006  $\alpha$ -Melanocyte-stimulating hormone and oxytocin: a peptide signalling cascade in the hypothalamus. *J Neuroendocrinol* 18:703–710
- Caqueneau C, Leng G, Guan XM, Jiang M, Van der Ploeg L, Douglas AJ 2006 Effects of  $\alpha$ -melanocyte-stimulating hormone on magnocellular oxytocin neurons and their activation at intromission in male rats. *J Neuroendocrinol* 18:685–691
- Sarkar S, Legradi G, Lechan RM 2002 Intracerebroventricular administration of  $\alpha$ -melanocyte stimulating hormone increases phosphorylation of CREB in TRH- and CRH-producing neurons of the hypothalamic paraventricular nucleus. *Brain Res* 945:50–59
- Dhillon WS, Small CJ, Seal LJ, Kim MS, Stanley SA, Murphy KG, Ghatei MA, Bloom SR 2002 The hypothalamic melanocortin system stimulates the hypothalamo-pituitary-adrenal axis *in vitro* and *in vivo* in male rats. *Neuroendocrinology* 75:209–216
- Mountjoy KG, Mortrud MT, Low MJ, Simerly RB, Cone RD 1994 Localization of the melanocortin-4 receptor (MC4-R) in neuroendocrine and autonomic control circuits in the brain. *Mol Endocrinol* 8:1298–1308
- Kishi T, Aschkenasi CJ, Lee CE, Mountjoy KG, Saper CB, Elmquist JK 2003 Expression of melanocortin 4 receptor mRNA in the central nervous system of the rat. *J Comp Neurol* 457:213–235
- Balthasar N, Dalgaard LT, Lee CE, Yu J, Funahashi H, Williams T, Ferreira M, Tang V, McGovern RA, Kenny CD, Christiansen LM, Edelstein E, Choi B, Boss O, Aschkenasi C, Zhang CY, Mountjoy K, Kishi T, Elmquist JK, Lowell BB 2005 Divergence of melanocortin pathways in the control of food intake and energy expenditure. *Cell* 123:493–505
- Singru PS, Sanchez E, Fekete C, Lechan RM 2007 Importance of melanocortin signaling in refeeding-induced neuronal activation and satiety. *Endocrinology* 148:638–646
- Niimi M, Murao K, Taminato T 2001 Central administration of neuromedin U activates neurons in ventrobasal hypothalamus and brainstem. *Endocrine* 16:201–206
- Ozaki Y, Onaka T, Nakazato M, Saito J, Kanemoto K, Matsumoto T, Ueta Y 2002 Centrally administered neuromedin U activates neurosecretion and induction of *c-fos* messenger ribonucleic acid in the paraventricular and supraoptic nuclei of rat. *Endocrinology* 143:4320–4329

23. Hanada R, Teranishi H, Pearson JT, Kurokawa M, Hosoda H, Fukushima N, Fukue Y, Serino R, Fujihara H, Ueta Y, Ikawa M, Okabe M, Murakami N, Shirai M, Yoshimatsu H, Kangawa K, Kojima M 2004 Neuromedin U has a novel anorexigenic effect independent of the leptin signaling pathway. *Nat Med* 10:1067–1073
24. Timofeeva E, Baraboi ED, Richard D 2005 Contribution of the vagus nerve and lamina terminalis to brain activation induced by refeeding. *Eur J Neurosci* 22:1489–1501
25. Johnstone LE, Fong TM, Leng G 2006 Neuronal activation in the hypothalamus and brainstem during feeding in rats. *Cell Metab* 4:313–321
26. Hiroyama M, Aoyagi T, Fujiwara Y, Birumachi J, Shigematsu Y, Kiwaki K, Tasaki R, Endo F, Tanoue A 2007 Hypermetabolism of fat in V1a vasopressin receptor knockout mice. *Mol Endocrinol* 21:247–258
27. Aoyagi T, Birumachi J, Hiroyama M, Fujiwara Y, Sanbe A, Yamauchi J, Tanoue A 2007 Alteration of glucose homeostasis in V1a vasopressin receptor-deficient mice. *Endocrinology* 148:2075–2084
28. Koshimizu TA, Nasa Y, Tanoue A, Oikawa R, Kawahara Y, Kiyono Y, Adachi T, Tanaka T, Kuwaki T, Mori T, Takeo S, Okamura H, Tsujimoto G 2006 V1a vasopressin receptors maintain normal blood pressure by regulating circulating blood volume and baroreflex sensitivity. *Proc Natl Acad Sci USA* 103:7807–7812
29. Shalev U, Highfield D, Yap J, Shaham Y 2000 Stress and relapse to drug seeking in rats: studies on the generality of the effect. *Psychopharmacology (Berl)* 150:337–346
30. McKinley MJ, Allen AM, Mathai ML, May C, McAllen RM, Oldfield BJ, Weisinger RS 2001 Brain angiotensin and body fluid homeostasis. *Jpn J Physiol* 51:281–289
31. Samson WK, White MM, Price C, Ferguson AV 2007 Obestatin acts in brain to inhibit thirst. *Am J Physiol Regul Integr Comp Physiol* 292:R637–R643
32. Iguchi H, Ikeda Y, Okamura M, Tanaka T, Urashima Y, Ohguchi H, Takayasu S, Kojima N, Iwasaki S, Ohashi R, Jiang S, Hasegawa G, Ioka RX, Magoori K, Sumi K, Maejima T, Uchida A, Naito M, Osborne TF, Yanagisawa M, Yamamoto TT, Kodama T, Sakai J 2005 SOX6 attenuates glucose-stimulated insulin secretion by repressing PDX1 transcriptional activity and is down-regulated in hyperinsulinemic obese mice. *J Biol Chem* 280:37669–37680

*Endocrinology* is published monthly by The Endocrine Society (<http://www.endo-society.org>), the foremost professional society serving the endocrine community.